International Journal of Pharmaceutics 376 (2009) 195–203

Contents lists available at ScienceDirect

International Journal of Pharmaceutics

journal homepage: www.elsevier.com/locate/ijpharm

Pharmaceutical Nanotechnology

Optimization of epirubicin nanoparticles using experimental design for enhanced intravesical drug delivery

Li-Ching Chang[a], Shu-Chin Wu[b], Jen-Wei Tsai[c], Tsan-Jung Yu[d], Tong-Rong Tsai[b,*]

[a] Department of Occupational Therapy, I-Shou University, Kaohsiung, Taiwan
[b] Faculty of Pharmacy, Kaohsiung Medical University, 100 Shih-Chuan 1st Road, Kaohsiung 807, Taiwan
[c] Department of Pathology, E-Da Hospital, Kaohsiung, Taiwan
[d] Department of Urology, E-DA Hospital/I-Shou University, Kaohsiung, Taiwan

ARTICLE INFO

Article history:
Received 8 March 2009
Received in revised form 22 April 2009
Accepted 25 April 2009
Available online 9 May 2009

Keywords:
Epirubicin
Nanoparticles
Bladder cancer
Intravesical instillation

ABSTRACT

The aim of this study was to develop poly(ethyl-2-cyanoacrylate) (PECA) epirubicin-loaded nanoparticles (EPI-NP). A 2^3 factorial design was adopted with the type of surfactant, surfactant concentration and the pH of the polymerization medium as independent variables. The particle size, entrapment efficacy and polydispersity index of eight formulations were then evaluated. Two optimal EPI-NP formulations, 2% Tween 80 EPI-NP (TW80 EPI-NP) and 0.5% pluronic F68 EPI-NP (F68 EPI-NP) at pH 2.5 were developed. The sizes of TW80 EPI-NP and F68 EPI-NP at maximum intensity were 90 and 220 nm, respectively. Both TW80 EPI-NP and F68 EPI-NP showed potent cytotoxicity against human bladder cancer T24 and RT4 cells, compared with aqueous solutions of epirubicin (EPI-AQ). The penetration and accumulation of EPI-NPs in pig urothelium were studied by tissue concentration-depth profiles and fluorescence microscopy. The cumulative amounts of epirubicin following EPI-AQ, TW80 EPI-NP and F68 EPI-NP treatments were 842.48 ± 24.66, 1314.66 ± 33.07 and 595.21 ± 24.16 μg, respectively. The current study showed the successful development of urothelium adhesive and penetrative PECA EPI-NPs. This has potential for the *in vivo* application of epirubicin-loaded nanoparticles for intravesical instillation in bladder cancer therapy.

1. Introduction

Intravesical administration is extensively adopted in treatment of patients with superficial bladder cancer. The initial treatment of non-muscle-invasive bladder cancer (NMIBC) is transurethral resection of the bladder tumour (TURBT). After TURBT, patients receive adjuvant instillations of chemotherapy or immunotherapy to lower the (high) recurrence rate and to prevent or delay progression to muscle-invasive disease. With immediate instillation after TURBT, the risk of recurrence in patients with NMIBC was about 50% at 2 yr and 15% at 5 yr (Sylvester et al., 2004). For patients with NMIBC, early instillation chemotherapy with epirubicin or mitomycin C after the TURBT is a safe and effective method that reduces the risk of recurrence in the short term but efficacy is only marginal in the long term. Sixty percent of patients who were treated with intravesical epirubicin regimens following TURBT and 41% of control subjects who underwent TURBT only, remained free of recurrences over a mean follow-up period of 32.9 months (Melekos et al., 1993). The risk-adapted first-line adjuvant therapy for NMIBC after TURBT is well established but has its limitations because the progression rate and high recurrence rate are problems for patients even following adjuvant intravesical chemotherapy or immunoprophylaxis (Lum and Torti, 1991; Witjes and Hendricksen, 2008).

The current formulation of epirubicin instilled in the bladder is a lyophilized powder dissolved in normal saline. However, this vehicle, when used in the intravesical administration of epirubicin, fails to provide sustained exposure to the urothelium. Thickened membrane plaques at the luminal surface and tight junctions are responsible for low permeability of the bladder urothelium, an important obstacle to the success of intravesical drug delivery (Tyagi et al., 2006). Strategies for improving intravesical therapy include increasing permeability and the residence time in the bladder using physical and chemical enhancement methods (Bogataj et al., 1999).

Factorial designs are commonly adopted in pharmaceutical research that is concerned with the effects of formulation variables and their interactions on response variables, because it yields the most information from the fewest experiments (Vandervoort and Ludwig, 2002). The major goals in designing nanoparticles as

Abbreviations: PECA, poly(ethyl-2-cyanoacrylate); DSC, differential scanning calorimetry; PBS, phosphate buffer saline.

* Corresponding author. Tel.: +886 7 3121101x2656; fax: +886 7 3210683.
E-mail address: changlc@isu.edu.tw (T.-R. Tsai).

0378-5173/$ – see front matter © 2009 Elsevier B.V. All rights reserved.
doi:10.1016/j.ijpharm.2009.04.045

a delivery system are to control particle size, surface properties and release of pharmacologically active agents to achieve a site-specific action of the drug at the therapeutically optimal rate and dose regimen (Mohanraj and Chen, 2006). In this work, DOE is utilized because it is highly sensitive to interactions of two or three factors, explaining their effects on the characteristics of epirubicin nanoparticles.

Nanoparticles are particularly useful in the delivery of drugs because their small size maximizes absorption and bioavailability. However, their small size and large surface area can lead to particle–particle aggregation and result in limited drug loading and burst release. Poly(alkylcyanoacrylate) (PACA) nanoparticles make good drug delivery systems because of their mechanical properties, biodegradability, high biocompatibility, drug compatibility and permeability (Fattal et al., 1997). Poly(ethyl-2-cyanoacrylate) (PECA) nanoparticles are biocompatible and mucoadhesive biopolymers, which form strong bonds with most polar substrates, including tissues and skin (Leonard et al., 1996). The preparation conditions of PECA nanoparticles, such as pH value and surfactant concentration, influence the particle size and the polymer molecular weight (Puglisi et al., 1993). Accordingly, biodegradable PECA was selected herein as a drug carrier.

The goal of this work was to develop and optimize epirubicin-loaded nanoparticles (EPI-NP) for intravesical instillation for use in place of the current aqueous formulation. The efficacy of drugs used in intravesical therapy is expected to increase with the duration of direct contact between the drug and the urothelium. In this study, EPI-NP was prepared by emulsion polymerization, with PECA as a carrier, and the optimized formulation was identified using a 2^3 factorial design. The factorial design used surfactant type, surfactant concentration and polymerization medium pH as the independent variables; and the particle size, entrapment efficacy and polydispersity index of eight formulations were characterized. The particle morphology was examined using transmission electron microscopy (TEM) and the amorphous and crystalline phases were elucidated using differential scanning calorimetry (DSC). The cytotoxicity of EPI-NP and its histological effects were determined to assay its potential for effective drug delivery. The adhesion of EPI-NPs to pig bladder urothelium and their penetration through the urothelium were assessed using modified Franz diffusion cells and fluorescent microscopy, and the cumulative doses were determined. This study identified the optimal ingredients for urothelium-adhesive and -penetrative PECA-emulsified EPI-NPs with potent biologically activity that can be exploited in intravesical instillation.

2. Materials and methods

2.1. Materials

Epirubicin was obtained from Calbiochem (La Jolla, CA). The monomers ethyl 2-cyanoacrylate and doxorubicin were purchased from Sigma Chemical Co. (St. Louis, MO, USA). Tween 80 was obtained from ICI Surfactants (Eversberg, Belgium), and Poloxamer 188 (F68) was obtained from BASF (Montreal, Canada). All organic solvents were of HPLC grade. All other chemicals were of reagent grade. Deionized water was purified using a Milli-Q system (Millipore, Milford, MA, USA). All cell culture medium and reagents were purchased from Gibco BRL (Grand Island, NY, USA). Most of the other chemical reagents were purchased from either Merck (Darmstadt, Germany) or Sigma–Aldrich.

Table 1
Experimental conditions for the factorial design parameters.

Factors	Levels	
	Low	High
(A) Surfactant type	Tween 80	F68
(B) Surfactant concentration	0.5%	2%
(C) The pH value of the polymerization medium	2	4

2.2. HPLC analysis of epirubicin

Epirubicin was analyzed with by HPLC with fluorescence detection (FLD). HPLC-FLD analyses were carried out using a model 510 solvent delivery system (Waters, Milford, MA), Waters 2475 Multi λ Fluorescence detector and Millennium version 4.0 software. An Acclaim®120 (150 mm × 4.6 mm ID) (Dionex, Surrey, UK) column used for separation of EPI. The mobile phase consisted of acetonitrile:0.1 M orthophosphoric acid:triethylamine:water at volumetric ratios 27:3:0.07:70 with an apparent pH of 2.8. The flow rate of the mobile phase was 1.0 mL/min. Doxorubicin was used as an internal standard. The column outlet stream was monitored at λEx-474 nm and λEm-551 nm.

2.3. Preparation of epirubicin nanoparticles using a factorial design

Poly(ethyl-2-cyanoacrylate) (PECA) nanoparticles loaded with epirubicin were prepared by emulsion polymerization. Experimental conditions for the factorial design parameters are shown in Table 1. Briefly, 1% (v/v) ethyl 2-cyanoacrylate monomer was added dropwise into a polymerization medium containing 0.1% epirubicin and poloxamer 188 (F68) (0.5% or 2% w/v) or Tween 80 (0.5% or 2% w/v) and processed as for dispersion polymerization (Harivardhan and Murthy, 2003). After 4 h, the mixture was neutralized with 0.1N NaOH, filtered through a sintered glass funnel (grade 3, pore size 20–30 μm) and freeze-dried after addition of 3% mannitol as a cryoprotector.

2.4. Experimental design and optimization of epirubicin nanoparticles

A 2^3 full factorial design was constructed for the epirubicin nanoparticles and 8 formulations (F1–F8) were selected using Design Expert software (Table 2). The three independent variables

Table 2
Matrix of the 2^3 factorial design and the responses of epirubicin nanoparticles.

Formulation code	Independent variables			Dependent variables		
	Surfactant type	Surfactant concentration	pH value	Particle size (nm)[a]	Entrapment efficacy (%)	Polydispersity index (PI)[a]
Fl	F68	0.5%	4	280.4 ± 0.73	47.80	0.114 ± 0.034
F2	F68	2.0%	4	272.8 ± 1.62	35.76	0.060 ± 0.018
F3	Tween 80	0.5%	2	101.6 ± 5.64	66.29	0.604 ± 0.166
F4	F68	2.0%	2	227.0 ± 0.84	65.21	0.077 ± 0.050
F5	Tween 80	0.5%	4	183.0 ± 18.88	40.26	0.996 ± 0.037
F6	Tween 80	2.0%	4	176.0 ± 4.23	48.31	0.910 ± 0.077
F7	Tween 80	2.0%	2	96.0 ± 4.29	68.43	0.583 ± 0.132
F8	F68	0.5%	2	242.0 ± 1.13	67.77	0.089 ± 0.046

[a] Mean ± S.D., $n = 6$.

were surfactant type (A), surfactant concentration (B) and pH of the polymerization medium (C). The characteristics of interest were particle size, entrapment efficacy and polydispersity index (PI), chosen in the design of the experiments as dependent variables. Based on the data thus obtained, the effects of variables A, B, and C separately, two-factor combinations AB, AC or BC, and all three factors together, ABC, were analyzed using the Design Expert software. The results are presented as half-normal probability plots, showing the percentage probability (y-axis) of the occurrence of the effects given in the x-axis, with particle size or entrapment efficacy as responses. The percentage of the probability P is given as the area under the curve of the percentage occurrence versus effect. If P is plotted against x, a sigmoid cumulative normal curve is obtained and when normal probability paper is used, with adjusted x- and y-axes, the P versus x plot is a straight line (Ročak et al., 2002).

2.5. Characterization of epirubicin nanoparticles

2.5.1. Determination of drug encapsulation efficacy

To determine the yield of epirubicin nanoparticles, an appropriate volume of each nanoparticle preparation was transferred into a centrifugal filter device (Microcon®, 100.000 NMWL, Millipore, USA) and centrifuged for 20 min at 12,000 rpm. One hundred microliters of clear filtrate was carefully withdrawn and diluted with methanol. The concentration of free epirubicin in the filtrate was determined by the above-mentioned HPLC method. The encapsulation efficacy of epirubicin nanoparticles was determined using the method of Wu et al. (2008) and is given by the equation,

$$\text{encapsulation efficacy}\,(\%) = \frac{C_e V_e - F_e V_e}{C_e V_e} \times 100$$

where C_e is the concentration of epirubicin in the epirubicin nanoparticles; V_e is the volume of epirubicin nanoparticles, and F_e is the concentration of un-encapsulated free epirubicin in the filtrate.

2.5.2. Particle size and polydispersity index analysis

The mean particle size and polydispersity index (PI) of the epirubicin nanoparticles were determined by photon correlation spectroscopy (N5 Submicron Particle Sizer analysis, BECKMAN COULTER®, USA) before freeze-drying. The formulations were diluted with double-distilled water for the measurements. The PI was used as a measure of the unimodal size distribution. A small value of PI indicates a homogenous population, while a large PI indicates a higher heterogeneity (Verma et al., 2003).

2.5.3. Zeta potential measurement

The zeta potential of nanoparticles was measured in a Malvern Zetasizer 3000 HSA (Malvern Instruments), with nanoparticles dispersed in phosphate-buffered saline (pH 7.4).

2.5.4. Differential scanning calorimetry

Differential scanning calorimetry (DSC) experiments were carried out to determine the possible interactions between epirubicin and excipients and to determine in which crystalline state epirubicin HCl was present in the particles. The thermograms of pure materials and lyophilized epirubicin-loaded nanoparticles were determined using a DSC-7 (Perkin-Elmer, Norwalk, CT). Approximately 3 mg of each sample was heated in aluminum pans from 150 to 230 °C and the scanning rate was conducted at 2 °C/min. An empty aluminum pan was used as a reference standard. Analysis was carried out under a nitrogen purge.

2.5.5. Transmission electron microscopy

Morphological evaluations of the EPI-loaded nanoparticles were performed using transmission electron microscopy (TEM) (JEOL JEM-2000 EXII TEM, Tokyo, Japan) following negative staining with 0.5% (w/v) phosphotungstic acid solution and fixing on copper grids for observation. Twenty milliliters of the original solution containing nanoparticles was diluted to 5 mL in buffer to obtain a clear solution and the samples for TEM were prepared using this.

2.6. Cytotoxicity and permeability of epirubicin nanoparticles

2.6.1. Cell culture

T24 and RT4 human bladder cancer cell lines were cultured in RPMI-1640 and McCoy's 5a medium (Gibco, Glasgow, United Kingdom) supplemented with 10% fetal bovine serum (FBS; Hyclone, Logan, UT, USA) and 10,000 units/mL of penicillin/streptomycin (Gibco BRL) at 37 °C in a humidified atmosphere of 5% CO_2 and 95% air.

2.6.2. Cell growth inhibition assay

Cell viability was determined using an MTT (3-(4,5-dimethylthiazol-2-yl)-2,5-diphenyltetrazolium bromide) assay. T24 and RT4 cells were trypsinized, disaggregated through a pipette, and counted with a hemacytometer. The cells were seeded in 96-well plates (10^4 cells/well), allowed to attach overnight, and then treated with different concentrations of aqueous epirubicin solution (EPI-AQ), TW80 EPI-NP, and F68 EPI-NP. After 24-h incubation, 20 μL of MTT reagent at a concentration of 5 mg/mL was added to each well and the cells were incubated for an additional 4 h. The MTS tetrazolium assay (Promega, Madison, WI) was used to determine the cell viability according to the manufacturer's instruction. The cell-growth inhibition potency of EPI-AQ, TW80 EPI-NP and F68 EPI-NP were expressed as IC_{50} values, defined as the concentration of the drug necessary to inhibit the growth of cells by 50%. Data are the means ± S.D. of four experiments (Chang et al., 1998).

2.6.3. Tissue preparation and permeability studies

An *in vitro* bladder permeability study was conducted with Yorkshire pig urinary bladders obtained from a local slaughterhouse and kept in PBS, cooled to 4 °C until use. All experiments were performed with a modified Franz diffusion assay (Kerec et al., 2005). The bladder corpus was cut into pieces (approximately 30 mm × 30 mm) and each piece was mounted into a Franz diffusion cell (Gauer Glas, Püttlingen, Germany) and the luminal side of the urinary bladder wall was exposed to equal volumes of 1.0 mg EPI-AQ, TW80 EPI-NP and F68 EPI-NP for 2 h. EPI-AQ, TW80 EPI-NP and F68 EPI-NP were poured off the tissue after permeability studies and the tissues were washed three times with PBS.

2.6.4. Histologic analysis

After the bladder permeability study, the remaining pig bladder tissue was fixed in formalin and embedded in paraffin for histological analysis. The histological analysis was carried out with hematoxylin and eosin (H&E) staining.

Table 3
The predicted and experimental response values for the optimized formulation of epirubicin nanoparticles.

	TW80 EPI-NP		F68 EPI-NP	
	Pred	Exp	Pred	Exp
Surfactant type	Tween 80	Tween 80	F68	F68
Surfactant concentration (%)	1.86	2	0.63	0.6
pH value	2.39	2.5	2.49	2.5
Particle size (nm)[a]	116.557	90.4 ± 3.4	247.512	245.9 ± 4.0
Entrapment efficacy (%)	61.39	63.19	61.32	57.28
Polydispersity index (PI)[a]	0.66	0.47 ± 0.08	0.08	0.05 ± 0.03
Zeta potential (mV)[a]		−24.5 ± 0.1		−27.7 ± 0.8
Drug content (μg/mL)		925.66		915.58

[a] Mean ± S.D., $n = 6$.

2.6.5. Determination of epirubicin in the bladder tissues

After permeability studies, pig urinary bladder tissue pieces with flat surfaces were sectioned by cryostat (LEICA CM 1900 Germany) in sections of 10 μm thickness parallel to the luminal surface up to 1.2 mm of the tissue depth (Kerec et al., 2005). Twenty consecutive sections were pooled into one sample and the weight determined. Epirubicin concentrations in the tissue were determined by HPLC.

(A)

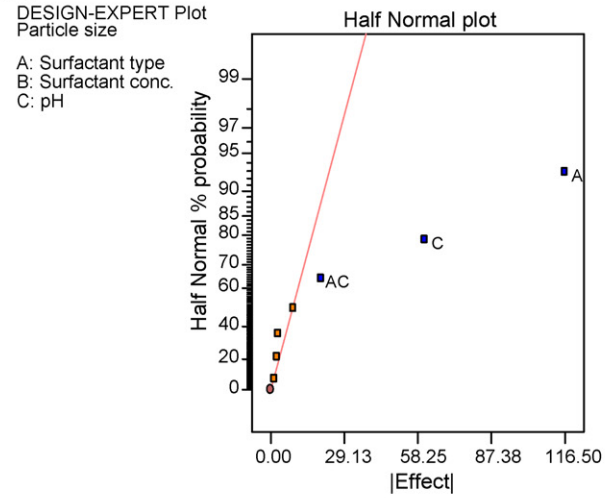

Source	d.f.	SS	MS	F	Prob>F
Particle size (nm) Mean=197.13		R^2 =0.9949	C.V.=3.42		
Model	3	35311.38	11770.46	259.40	< 0.0001
Surfactant type	1	23323.24	23323.24	514.01	< 0.0001
pH	1	7503.12	7503.12	165.36	0.0002
Surfactant type × pH	1	780.13	780.13	17.19	0.0143
Residual	4	181.50	45.38		
Total	7	35492.88			

(B)

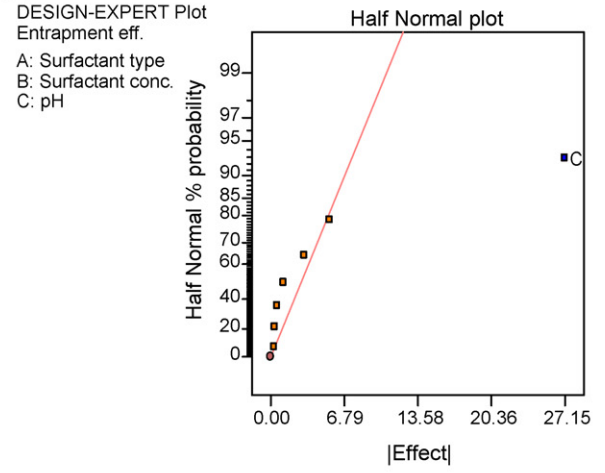

Source	d.f.	SS	MS	F	Prob>F
Entrapment Efficacy (%)	Mean=53.35	R^2 =0.9468	C.V.= 6.97		
Model	1	1474.25	1474.25	106.72	<0.0001
pH	1	1474.25	1474.25	106.72	<0.0001
Residual	6	82.89	13.81		
Total	7	1557.13			

SS, sum of squares; d.f., degrees of freedom; MS, Mean square
*Prob > F less than .05 indicate model terms are significant.

Fig. 1. Half-normal probability plots of epirubicin nanoparticles. The particle size (A) and entrapment efficacy (B) were examined with variable factors comprising surfactant type, surfactant concentration and medium pH.

2.7. Statistical data analysis

All data were expressed as means ± standard deviations. Statistically significant differences were determined using the Student's *t*-test with $P < 0.05$ as a minimal level of significance.

3. Results and discussion

3.1. Characterization of epirubicin nanoparticles (EPI-NP)

A 2^3 factorial design was used experimentally to test the effect of the three factors: surfactant type, surfactant concentration and pH of the polymerization medium in the preparation of PECA emulsified EPI-NP. Table 2 shows eight experimental runs (F1–F8) using Design Expert software to accommodate three factors with two levels. The particle sizes of EPI-NP with Tween 80 as surfactant (F3, F5, F6, F7) ranged from 96.0 ± 4.29 to 183.0 ± 18.88 nm, whereas the sizes of EPI-NP with F68 as surfactant (F1, F2, F4, F8) ranged from 227.0 ± 0.84 to 280.4 ± 0.73 nm. The entrapment efficacy of formulations with Tween 80 as surfactant was 40.26–68.43% and that with F68 as surfactant was 35.76–67.77%. The PI reveals reasonable homogeneity of the nanoparticles and the PI values of Tween 80 and F68 as surfactants were 0.583 ± 0.132 to 0.996 ± 0.037 and 0.060 ± 0.018 to 0.114 ± 0.034, respectively.

The effect of pH on the formulation of the nanoparticles with Tween 80 as the surfactant is the clearest. With 2.0% Tween 80 as the surfactant, and the medium at pH 2 (F7) and pH 4 (F8), the sizes of the nanoparticles were 96.0 ± 4.29 and 176.0 ± 4.23 nm, the entrapment efficacies were 68.43% and 48.31%, and the PIs were 0.583 ± 0.132 and 0.910 ± 0.077, respectively. A possible explanation for the difference between the particle sizes is the difference between the extents of cross-linking at the two pH levels. If the cross-linking reaction is favored at a pH of 2, more cross-links would form, yielding a denser network and smaller particles (Vandervoort and Ludwig, 2002).

3.2. Determination of optimal formulations

The optimal formulations of epirubicin-loaded PECA nanoparticles were subject to factorial analysis. Fig. 1A and B presents the

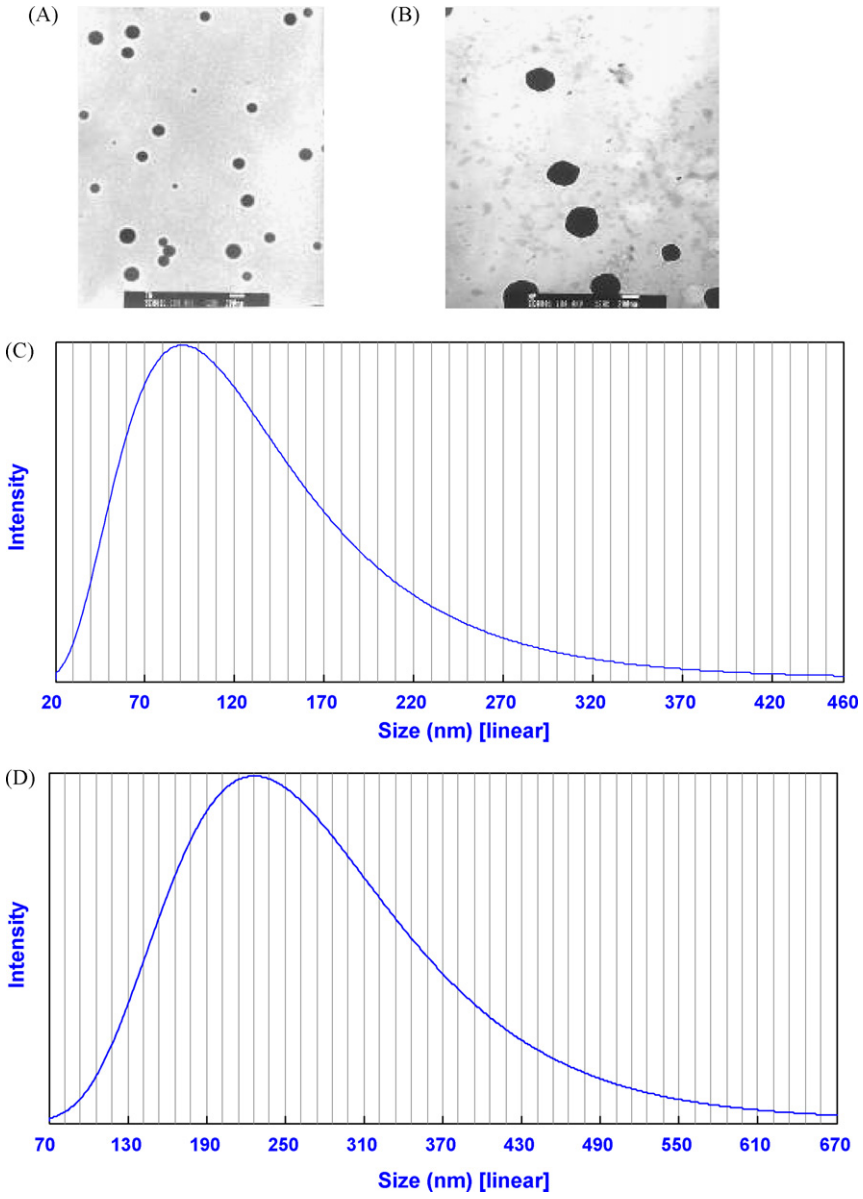

Fig. 2. TEM photographs and particle sizes of epirubicin nanoparticles. Particle morphology from TEM photographs of TW80 EPI-NP (A) and F68 EPI-NP (B). Particle size distributions of TW80 EPI-NP (C) and F68 EPI-NP (D).

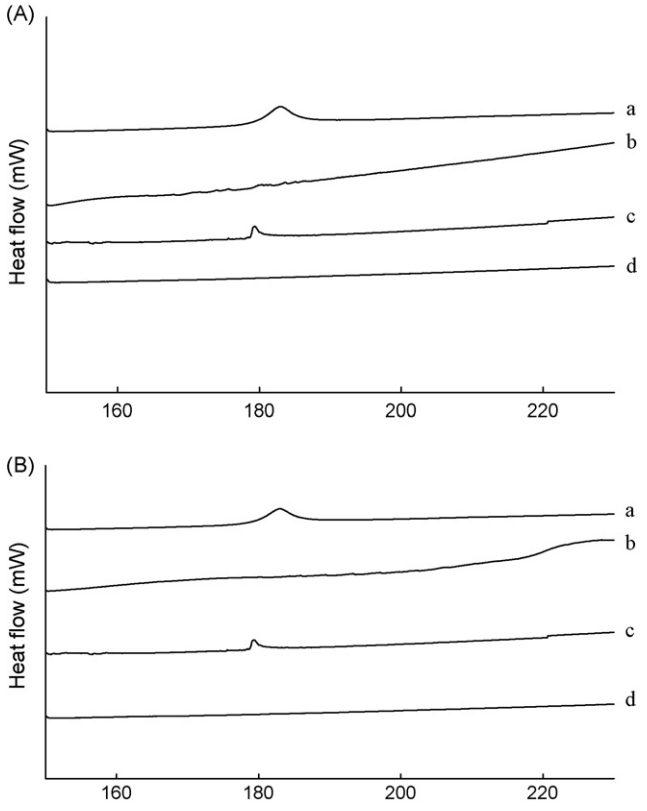

Fig. 3. DSC curves of epirubicin nanoparticles. DSC curves of TW80 EPI-NP (A) and F68 EPI-NP (B); a, epirubicin, b, lyophilized epirubicin-free NP; c, physical mixture, d, lyophilized TW80 EPI-NP in (A) or lyophilized F68 EPI-NP in (B).

main effects of parameters A, B and C, the combined factors AB, AC and BC and all three factors ABC together, on particle size and entrapment efficacy. The data were analyzed using ANOVA, and each parameter was evaluated using the *F* test. In Fig. 1A, the factors that predominantly determine the size of EPI-NP were the surfactant type (A), the pH (C) and these two factors together, AC. Importantly, the factor associated with the most distant point (surfactant type, A) from the fitted curve of the half-normal plot had a larger effect on particle size than did C, AC or the other factors. In Fig. 1B, the factor that significantly affected the entrapment efficacy of EPI-NP was the pH value (C).

Based on the above data, two formulations were optimized using the Design Expert software as follows (Table 3); 1.86% Tween 80 with a polymerization medium at pH 2.39 and 0.63% F68 with a medium pH of 2.49 (denoted Pred). Two modified formulations (denoted Exp), TW80 EPI-NP (2% Tween 80 with pH 2.5) and F68 EPI-NP (0.6% F68 with pH 2.5), were applied to confirm the predictions of the particle size, entrapment efficacy and PI. When the surfactant was Tween 80, the Pred and Exp particle sizes, entrapment efficacies and PIs were 116.557 and 90.4 ± 4.3, 61.39% and 63.19%, and 0.66 and 0.47 ± 0.08, respectively. When the surfactant was F68, the Pred and Exp particle sizes, entrapment efficacies and PIs were 247.512 and 245.9 ± 4.0, 61.32% and 57.28%, and 0.08 and 0.05 ± 0.03, respectively. The drug contents of TW80 EPI-NP and F68 EPI-NP in Exp conditions were 925.66 and 915.58 μg/mL. Hence, the experimental formulations of TW80 EPI-NP and F68 EPI-NP were consistent with the predicted values and were employed in subsequent studies.

The results of the Design Expert analysis of EPI-NP revealed that surfactant type had the greatest effect on particle size and the pH of the medium was the factor that most strongly affected drug loading and entrapment efficiency in the preparation of epirubicin-loaded PECA nanoparticles. The capacity of nanoparticles to change the biodistribution and pharmacokinetics of drugs has important *in vivo* therapeutic applications. In this respect, the size and surface characteristics of nanoparticles are crucial.

3.3. Morphology and particle size distribution

Particle size and size distribution determine the *in vivo* distribution, biological fate, toxicity and the targeting ability of nanoparticle systems. In addition, they can also influence the drug loading, drug release and stability of nanoparticles (Mohanraj and Chen, 2006). Fig. 2A and B presents the TEM analyses of the morphologies of TW80 EPI-NP and F68 EPI-NP particles. The TEM images reveal that the TW80 EPI-NPs were smaller spheres with more uniform size distributions than F68 EPI-NPs. In Fig. 2C and D, the particle sizes ranged from 20 to 480 nm for TW80 EPI-NP and from 70 to 670 nm for F68 EPI-NPs. The sizes associated with maximum intensity for TW80 EPI-NP and F68 EPI-NP were 90 and 220 nm, respectively.

3.4. Differential scanning calorimetry

DSC was performed to determine whether the epirubicin was incorporated into the nanoparticles in its crystalline or amorphous form and to elucidate the interaction of epirubicin with other ingredients. DSC curves of the EPI, TW80 EPI-NP and F68 EPI-NP are displayed in Fig. 3. The endothermic peak of EPI was obtained at 183 °C. However, the endothermic peak of epirubicin was com-

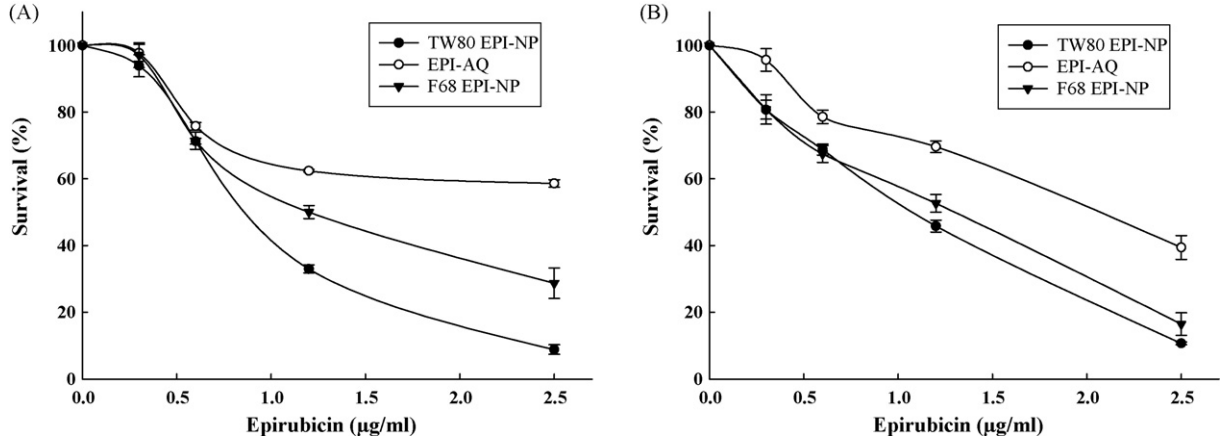

Fig. 4. The cytotoxicity of epirubicin nanoparticles against human bladder cancer cells. The epirubicin aqueous solutions (EPI-AQ), TW80 EPI-NP and F68 EPI-NP were incubated with human bladder cancer cell lines T24 (A) and RT4 (B) and the cytotoxicity was evaluated by MTS assay. Values were expressed as mean ± S.D., $n = 4$.

pletely absent from all lyophilized TW80 EPI-NP and F68 EPI-NP. These results suggest that the drug was dispersed throughout the polymers to form a high-energy amorphous state, which is more soluble in water than the crystalline state. The amorphous form, because of the absence of an ordered crystal lattice, requires the least energy and is more soluble than the crystalline or hydrated forms of a drug.

3.5. Cytotoxicity assay

Epirubicin is a chemotherapy drug currently used in the intravesical instillation for superficial bladder cancer. Thus, it was crucial to evaluate the cytotoxicity of epirubicin nanoparticle formulations. The effects of aqueous epirubicin solution (EPI-AQ), TW80 EPI-NP and F68 EPI-NP on the cell viability of human bladder cancer cell lines T24 (Fig. 4A) and RT4 (Fig. 4B) were determined by MTS assay. The EPI-AQ, TW80 EPI-NP and F68 EPI-NP caused 50% (IC_{50}) T24 cell death at concentrations of 25.85, 1.19 and 1.52 μg/mL, respectively (Fig. 4A). EPI-AQ, TW80 EPI-NP and F68 EPI-NP caused 50% (IC_{50}) RT4 cell death at concentrations of 2.00, 1.20 and 1.30 μg/mL, respectively (Fig. 4B). The cytotoxicity of TW80 EPI-NP and F68 EPI-NP toward both T24 and RT4 cells significantly exceeded that of EPI-AQ ($P < 0.05$).

Lipophilicity/hydrophilicity is important in determining the distribution and/or accumulation of tissue. Lu et al. (2004) noted that hydrophilic gelatin enhances the diffusion-mediated release of paclitaxel in paclitaxel-loaded gelatin nanoparticles. Paclitaxel has a very low aqueous solubility; its physical state in the gelatin matrix determines its rate of dissolution. The size of paclitaxel-loaded gelatin nanoparticles ranged from 600 to 1000 nm. In this study, the epirubicin is hydrophilic and PECA is a mucoadhesive drug carrier used in intravesical formulation development. The particle sizes of TW80 EPI-NP and F68 EPI-NP were 90.4 ± 3.4 nm and 245.9 ± 4.0 nm, respectively. A comparison of cytotoxicity to human bladder transitional cancer cells indicates that the IC_{50} concentrations of paclitaxel-loaded nanoparticles almost equal those of aqueous paclitaxel. However, the TW80 EPI-NP and F68 EPI-NP showed more cytotoxicity than EPI-AQ.

3.6. Permeability studies and histology examination

The rationale for using nanoparticles is based on their ability to deliver a concentrated dose of drug in the vicinity of the targets via the enhanced permeability and retention effect or active targeting by ligands on the surface of nanoparticles (Mohanraj and Chen, 2006). Fig. 5 presents the results of histological examinations using hematoxylin and eosin (H&E) staining of normal pig bladder and pig bladders subjected to aqueous epirubicin solution (EPI-AQ), TW80 EPI-NP and F68 EPI-NP after the permeability assay with a Franz diffusion cell. In normal bladder mucosa, the urothelium of the urinary bladder was intact with rounded surfaces of the umbrella cells. Following treatment with EPI-AQ, the umbrella and intermediate cells of urothelium were denuded. TW80 EPI-NP treatment caused the umbrella and intermediate urothelial cells mild loss of integrity at focal areas. After F68 EPI-NP treatment, only subtle denudation of the urothelium was discernible. Furthermore, H&E staining revealed no remarkable microscopic feature in the suburothelial stroma.

3.7. Tissue concentration–depth profiles

The efficacy of intravesical therapy for bladder cancer is in part limited by the poor penetration of drugs into the urothelium. In the present work, permeability studies were used to evaluate the efficacy of EPI-NP. Fig. 6A presents phase-contrast and paired fluorescence microscopic images of EPI-AQ, TW80 EPI-NP and F68 EPI-NP, showing the penetration following the 2 h *in vitro* Franz diffusion assay. Fluorescence microscopy revealed that the fluorescence of epirubicin that resulted from these three formulations is limited to the urothelium. Observation of the lumen side of the

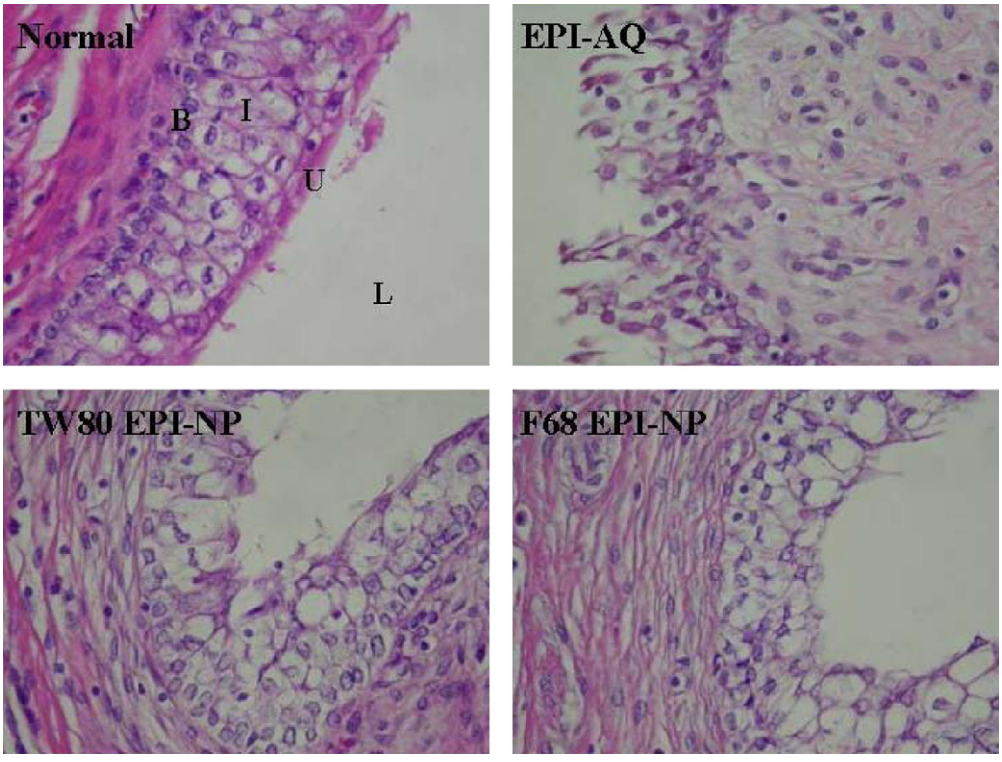

Fig. 5. Histopathology of pig bladder sections with hematoxylin and eosin (H&E) staining on untreated (normal) cells and cells treated with epirubicin aqueous solution (EPI-AQ), TW80 EPI-NP and F68 EPI-NP, at ×400 magnification. L, lumen; U, umbrella cells; I, intermediate cells; B, basal cells.

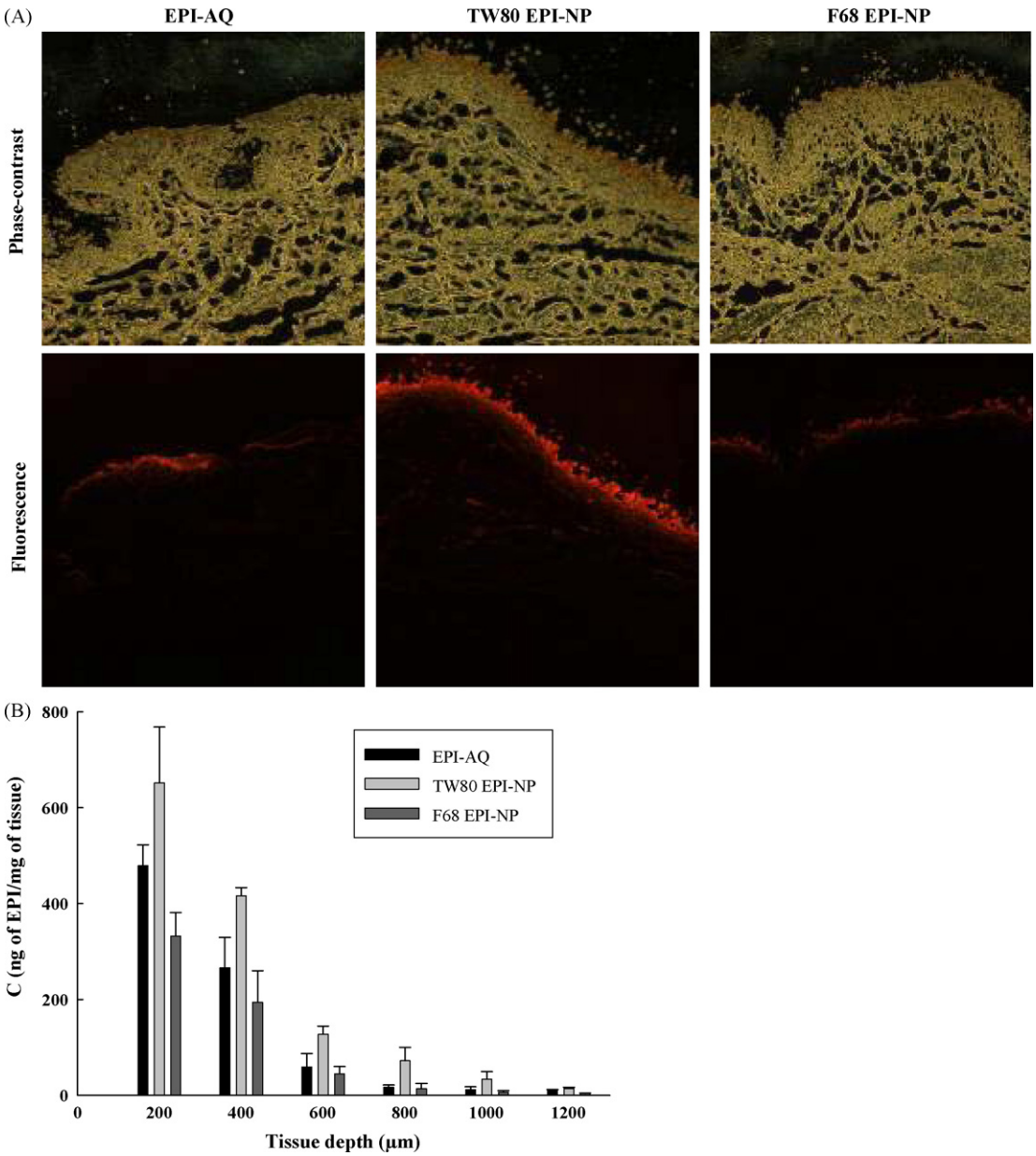

Fig. 6. Permeability of epirubicin nanoparticles (EPI-NP). (A) Phase contrast and fluorescent images of pig bladder cross-sections 2 h after EPI-AQ, TW80 EPI-NP and F68 EPI-NP treatment using Franz diffusion cells, at x200 magnification. (B) Amount of epirubicin (EPI) that permeated into the pig bladder wall as a function of tissue depth (Mean ± S.D., $n = 6$).

bladder indicated that the EPI-AQ exhibited little distributed fluorescence and limited penetration of the urothelium. The TW80 EPI-NP exhibited more homogeneous fluorescence and greater penetration intensity into the urothelium. The F68 EPI-NP fluoresced weakly and penetrated the pig bladder urothelium to a lesser extent. This investigation supports the assumption that the epirubicin-loaded nanoparticles with Tween 80 as surfactant are transferred more easily into the urothelium of bladder than aqueous epirubicin.

Fig. 6B presents the tissue concentration-depth profile of EPI-AQ, TW80 EPI-NP and F68 EPI-NP in the pig bladder wall following the Franz diffusion assay. The concentrations of epirubicin were normalized according to the weight of wet tissue. Tissue concentrations of epirubicin decreased as the tissue depth from the urothelium increased. At a depth of 200 μm from the apical urothelium, following EPI-AQ, TW80 EPI-NP and F68 EPI-NP treatment, the concentrations of epirubicin per mg of tissue were 478.76 ± 43.86, 651.59 ± 116.75 and 332.36 ± 49.00 μg/mg tissue, respectively. At a depth of 400 μm, the concentrations of epirubicin per mg of tissue were 266.40 ± 62.88, 416.33 ± 17.17 and 194.26 ± 65.74 μg/mg tissue, respectively. From 0 to 1200 μm from the apical urothelium, the cumulative amounts of epirubicin following EPI-AQ, TW80 EPI-NP and F68 EPI-NP treatments were 842.48 ± 24.66 μg, 1314.66 ± 33.07 μg, and 595.21 ± 24.16 μg, respectively.

4. Conclusions

The present study demonstrated that the epirubicin-loaded PECA nanoparticles system was successfully developed and presented rapidly released epirubicin. The epirubicin nanoparticles exhibit significant cytotoxicity in human bladder cancer cells and higher tissue concentrations compared with a commercial aqueous formulation. Biocompatible and mucoadhesive PECA polymers were used in emulsion polymerization of EPI-NP with the surfac-

tants Tween 80 (TW80 EPI-NP) and F68 (F68 EPI-NP). The optimal surfactant type and the medium pH value in the preparation of EPI-NPs were identified by a factorial design. TW80 EPI-NPs particles had a size smaller than 100 nm. Moreover, the potent cytotoxicity and urothelium penetration of TW80 EPI-NP may increase the efficacy of intravesical instillation over that of aqueous epirubicin. The data suggests that nanoparticles are potentially a useful epirubicin formulation for intravesical treatment of bladder cancer.

Acknowledgements

The authors would like to thank the National Science Council of the Republic of China, Taiwan (NSC97-2314-B-214-010) and I-Shou University (ISU97-04-08) for financial supporting of this research. Editorial assistance from Ted Knoy is appreciated.

References

Bogataj, M., Mrhar, A., Korosec, L., 1999. Influence of physicochemical and biological parameters on drug release from microspheres adhered on vesical and intestinal mucosa. Int. J. Pharm. 177, 211–220.

Chang, L.C., Tsai, T.R., Wang, J.J., Lin, C.N., Kuo, K.W., 1998. The rhamnose moiety of solamargine plays a crucial role in triggering cell death by apoptosis. Biochem. Biophys. Res. Commun. 242, 21–25.

Fattal, E., Roques, B., Puisieux, F., Blanco-Prieto, M.J., Couvreur, P., 1997. Multiple emulsion technology for the design of microspheres containing peptides and oligopeptides. Adv. Drug Deliv. Rev. 28, 85–96.

Harivardhan, R.L., Murthy, R.S.R., 2003. Polymerization of n-butyl cyanoacrylate in presence of surfactant: study of influence of polymerization factors on particle properties, drug loading and evaluation of its drug release kinetics. Ars. Pharma. 44, 351–369.

Kerec, M., Bogataj, M., Veranic, P., Mrhar, A., 2005. Permeability of pig urinary bladder wall: the effect of chitosan and the role of calcium. Eur. J. Pharm. Sci. 25, 113–121.

Leonard, F., Kulkarni, R.K., Brandes, G., Nelson, J., Cameron, J.J., 1996. Synthesis and degradation of poly(alkyl-α-cyanoacrylates). J. Appl. Polym. Sci. 10, 259–272.

Lu, Z., Yeh, T.K., Tsai, M., Au, J.L., Wientjes, M.G., 2004. Paclitaxel-loaded gelatin nanoparticles for intravesical bladder cancer therapy. Clin. Cancer. Res. 22, 7677–7684.

Lum, B.L., Torti, F.M., 1991. Adjuvant intravesicular pharmacotherapy for superficial bladder cancer. J. Natl. Cancer Inst. 83, 682–694.

Melekos, M.D., Chionis, H.S., Paranychianakis, G.S., Dauaher, H.H., 1993. Intravesical 4′-epi-doxorubicin (epirubicin) versus bacillus Calmette-Guérin. A controlled prospective study on the prophylaxis of superficial bladder cancer. Cancer 72, 1749–1755.

Mohanraj, V.J., Chen, Y., 2006. Nanoparticles—a review. Trop. J. Pharm. Res. 5, 561–573.

Puglisi, G., Giammona, G., Fresta, M., Carlisi, B., Micali, N., Villari, A., 1993. Evaluation of polyalkylcyanoacrylate nanoparticles as a potential drug carrier: preparation, morphological characterization and loading capacity. J. Microencapsul. 10, 353–366.

Ročak, D., Kosec, M., Degen, A., 2002. Ceramic suspension optimization using factorial design of experiments. J. Eur. Ceram. Soc. 22, 391–395.

Sylvester, R.J., Oosterlinck, W., van der Meijden, A.P., 2004. A single immediate postoperative instillation of chemotherapy decreases the risk of recurrence in patients with stage Ta T1 bladder cancer: a meta-analysis of published results of randomized clinical trials. J. Urol. 171, 2186–2190.

Tyagi, P., Tyagi, S., Kaufman, J., Huang, L., de Miguel, F., 2006. Local drug delivery to bladder using technology innovations. Urol. Clin. North Am. 33, 519–530.

Vandervoort, J., Ludwig, A., 2002. Biocompatible stabilizers in the preparation of PLGA nanoparticles: a factorial design study. Int. J. Pharm. 238, 77–92.

Verma, D.D., Verma, S., Blume, G., Fahr, A., 2003. Particle size of liposomes influences dermal delivery of substances into skin. Int. J. Pharm. 258, 141–151.

Witjes, J.A., Hendricksen, K., 2008. Intravesical pharmacotherapy for non-muscle-invasive bladder cancer: a critical analysis of currently available drugs, treatment schedules, and long-term results. Eur. Urol. 53, 45–52.

Wu, T.H., Yen, F.L., Lin, L.T., Tsai, T.R., Lin, C.C., Cham, T.M., 2008. Preparation, physicochemical characterization, and antioxidant effects of quercetin nanoparticles. Int. J. Pharm. 346, 160–168.